Acta Materialia 125 (2017) 303–310

Contents lists available at ScienceDirect

Acta Materialia

journal homepage: www.elsevier.com/locate/actamat

Full length article

Particle-induced morphological modification of Al alloy equiaxed dendrites revealed by sub-second *in situ* microtomography

R. Daudin [a, *], S. Terzi [b, c], P. Lhuissier [a], J. Tamayo [d], M. Scheel [c, e], N. Hari Babu [d], D.G. Eskin [d], L. Salvo [a]

[a] Univ. Grenoble Alpes, CNRS, SIMAP, F-38000, Grenoble, France
[b] European Space Agency, ESTEC, TEC-TS, EPN Campus, CS20156, 38042, Grenoble Cedex 9, France
[c] ESRF-The European Synchrotron, CS40220, 38043, Grenoble Cedex 9, France
[d] Brunel Centre for Solidification Technology, Brunel University London, Uxbridge, UB8 3PH, UK
[e] Société Civile Synchrotron SOLEIL, Saint-Aubin - BP 48, 91192, Gif-sur-Yvette Cedex, France

ARTICLE INFO

Article history:
Received 24 August 2016
Received in revised form
1 December 2016
Accepted 4 December 2016

Keywords:
Al alloys
Metal matrix composites (MMCs)
Synchrotron radiation computed tomography
Solidification microstructures
Equiaxed dendrites morphologies

ABSTRACT

The study of dendritic growth is a challenging topic at the heart of intense research in material science. Understanding such processes is of prime importance as it helps predicting the final microstructure governing material properties. In the specific case of the design of metal-matrix nanocomposites (MMNCs), the addition of nano-sized particles inside the metallic melt increases the complexity as their influence on the growth morphology of dendrites is not yet fully understood. In the present experimental study, we use *in situ* X-ray tomography imaging with very high temporal resolution (0.35 s per 3D image) coupled with *in situ* ultrasonic melt homogenisation to record, in 3D and real time, the free growth at high cooling rates (~2 K s^{-1}) of equiaxed dendrites in an aluminium-based alloy (AA6082) containing Y_2O_3 nanoparticles. The careful 3D analysis of the dendrite morphologies as well as their solidification dynamics reveals that in the case of well-dispersed particles, dendrite equiaxed growth occurs through complex hyper-branched morphologies. Such behaviour is believed to arise from particle-induced modification of the solidification processes at the origin of multiple splitting, branching and curving mechanisms of the dendrite arms. These results shed light on long-standing empirical and modelling statements and open new ways for direct investigation of equiaxed growth in metallic alloys and composites.

1. Introduction

Describing and understanding accurately the complexity and the diversity of dendrites morphologies is a challenging fundamental physical problem related to liquid-solid phase transition [1] and is of high practical interest as it helps predicting the final microstructure that governs the materials properties.

Many models have been derived and completed over the years to describe the steady-state dendrite growth, from the early analytical model of Ivantsov [2] to the recent multiscale dendritic needle network model [3,4] and the widely used phase field approach [5–9]. Until recently, only transparent organics that are thought to “freeze like metals” [10] could be used as experimental validation but could only provide 2D observations [11–13] and recent outcomes pointed out that metallic alloys may present more complex behaviour [8,14]. Because of technical issues concerning the time needed to collect images *in situ*, free growth stages are mainly accessible by radiography (2D) [4,15–17] and X-ray tomography (3D) is often limited to slow cooling rates [14,18–20]. Very few studies report *in situ* tomography acquisition during dendrites free growth at relatively high cooling rates [21–23]. While our understanding on dendrites growth is constantly improving, most advanced models or simulation techniques still cannot fully describe experimental results [24] and lack 3D *in situ* experimental dataset in metals to be improved.

For more complex materials, such as metal-matrix nanocomposites (MMNCs) that are promising materials in applications where lightweighting and high strength are important issues [25], interaction between the solidification front and the particles requires consideration. If a consensus seems to exist for a planar front

* Corresponding author.
E-mail address: remi.daudin@simap.grenoble-inp.fr (R. Daudin).

http://dx.doi.org/10.1016/j.actamat.2016.12.005
1359-6454/

interfering with a spherical particle [26–28], only few studies focus on dendrite tips and particles interactions [6,11,29]. Using 2D phase field simulations, Granazy et al. showed that particles can significantly modify the equiaxed dendrites morphology [6,7]. Experimental evidence of such mechanisms in metals, in 3D, is missing mainly due to the fact that natural aggregation of the particles in the melt hinders clear comparison [18]. The size of aggregates can be significantly reduced by applying intense ultrasonic melt treatment (UST) leading to an excellent dispersion of particles within the melt prior to solidification [26,30,31]. By adapting this technique on a synchrotron tomography beamline, we managed to observe experimentally in 3D the free growth of equiaxed dendrites in a liquid AA6082 alloy containing Y_2O_3 nanoparticles. We show that the size and the distribution variations of the nanoparticles lead either to dense globular or complex hyper-branched dendrites. These experimental results are confronted to reported numerical works [6–8,29,32] and provide valuable insights for crystal growth and development of low-alloy Al MMNCs.

2. Experimental methods

2.1. Sample preparation

The material was processed by BCAST at Brunel University London. The incorporation of 1 wt% Y_2O_3 particles (~500 nm) in the molten AA6082 Al-based alloy (composition in wt%: 0.7–1.3% Si, 0.4–1% Mn, 0.6–1.2% Mg, 0.5% Fe, 0.25% Cr, 0.2% Zn, 0.1% Cu, 0.1% Ti.) matrix was performed under mechanical stirring (Ti impeller at 400 rpm). Ultrasonic melt treatment was applied for 5 min at a frequency of 17.5 kHz with a Nb sonotrode (amplitude nul-to-peak of 20 μm). The detailed procedure can be found elsewhere [33]. The samples were machined into cylindrical-shaped specimens of 5 mm in diameter fitting to the crucible inside which they were further melted.

2.2. Experimental apparatus

The sonication device is composed of a transducer, a booster and a sonotrode. Both transducer and booster are commercially available parts (MPI-ultrasonics) whereas the probe part was especially designed to efficiently apply ultrasound to molten millimetre-size Aluminium composite samples during *in situ* tomography imaging (Fig. 1). The system is based on a principle where the fine sonotrode is introduced inside a small crucible. Whereas conventional designs for large sonotrodes usually include probes composed of one or two sections, the present sonotrode is composed of three different sections. Indeed, the reduction of the tip diameter increases the constraints at the reduction section leading to failure after short time of use. Using COMSOL software, a three-section sonotrode was modelled for a targeted eigenfrequency of 20 kHz using a two dimensional axisymmetric approach. The total length (145 mm) and the different lengths corresponding to the different sections with fixed diameters (12, 6 and 3 mm) were computed by minimizing and balancing the stresses along the ultrasonic horn. The Ti sonotrode was then machined at the lab according to the computational results obtained. The crucibles containing the 5 mm samples are made of alumina and were glued at the top of an alumina rod fixed on a rotating stage. An induction furnace consisted of a copper coil placed around the crucible allowing the samples to be remelted. The temperature was measured using a pyrometer monitoring the area imaged during solidification. The sonotrode was screwed on the sonication device that was mounted on a translation stage above the crucible. The vertical displacement of the ultrasonic horn was remotely controlled allowing its immersion inside the melt for ultrasonic treatments and its withdrawing quickly after US processing. The frequency, amplitude and duration of ultrasounds were controlled using an MPI Labview program.

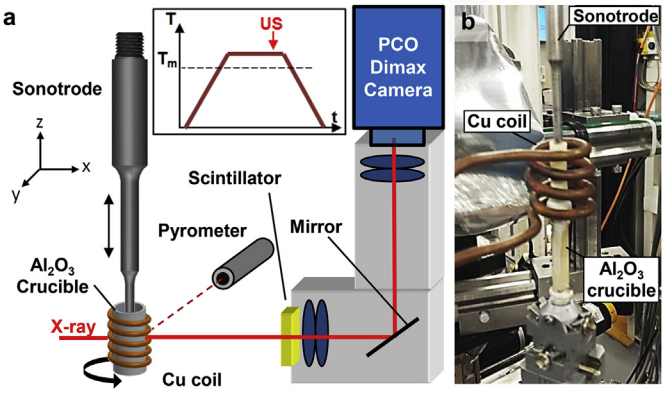

Fig. 1. Experimental apparatus. a Schematic drawing of the experimental device. Inset shows the thermal treatment applied to the samples (T_m is the melting temperature). When performed, UST were applied in the fully liquid state. **b** Picture of the experimental equipment.

2.3. Experimental procedure

The experimental procedure consisted in three stages. First, a AA6082 Al alloy either containing or not Y_2O_3 nanoparticles was melted with an induction furnace. Second, in the fully liquid state, ultrasonic treatment (30 s at a frequency of 19.6 kHz) was either applied or not through the dedicated Ti sonotrode. Finally, the sonotrode was withdrawn, the induction furnace switched off letting the sample cool naturally and ultrafast *in situ* microtomography was performed. The unique combination of high energy and high flux provided by the ESRF-ID15 beamline enables the examination of the complete solidification sequence inside 5 mm thick samples at cooling rates in between 1.5 and 3 K s^{-1}. The time range during which useful information on free growth mechanisms was accessible was very short (~1.5 s) but sufficient to unravel the impact of UST on the size and distribution of Y_2O_3 nanoparticles and consequently on the dendrite growth morphologies. Additional results regarding samples without nanoparticles are discussed in Supplementary Material.

2.4. In situ tomography data acquisition

In situ tomography was performed at the ID15 beamline at ESRF during solidification after ultrasonic melt treatment. A dedicated optic system composed of an ×10 objective and a LuAG scintillator converting the X-ray light into visible light were placed at front of the camera. The latter was a PCO-Dimax camera allowing ultrafast acquisition of images. The tomography scans were recorded during the solidification of the sample from the liquid state. The induction furnace was powered down right after and continuous acquisition was performed during solidification with a cooling rate of the order of 2 K s^{-1} by recording 52000 projections with an exposure time of 0.35 ms, a pixel size of 1.1 μm and a field of view of 1200 × 400 voxels (1.32 × 0.44 mm^3). The angular projection step was set to record 1000 images over 180° leading to a scan time of 0.35s. Continuous acquisition was performed meaning that there was no delay between two scans. 52 scans were recorded in the camera memory leading to 32 Gb of data. Data was then downloaded from camera memory to disks while another sample was mounted.